FORMATION MECHANISM OF GRAPHITE HEXAGONAL PYRAMIDS BY ARGON PLASMA ETCHING OF GRAPHITE SUBSTRATES

X. Glad, L. de Poucques, J. Bougdira

FORMATION MECHANISM OF GRAPHITE HEXAGONAL PYRAMIDS BY ARGON PLASMA ETCHING OF GRAPHITE SUBSTRATES

*X. Glad[1,2], L. de Poucques[*1,2], J. Bougdira[1,2].*

[1]Université de Lorraine, Institut Jean Lamour UMR 7198, Vandœuvre-lès-Nancy, F-54506, France.

[2]CNRS, Institut Jean Lamour UMR 7198, Vandœuvre-lès-Nancy, F-54506, France.

ABSTRACT–

A new graphite crystal morphology has been recently reported, namely the graphite hexagonal pyramids (GHPs). They are crystals of hexagonal habit with diameters ranging from 50 to 800 nm and a constant apex angle of 40°. These nanostructures are formed from graphite substrates (flexible graphite and highly ordered pyrolytic graphite) in low pressure helicon coupling radiofrequency argon plasma at 25-eV ion energy and, allegedly, due to a physical etching process. In this paper, the occurrence of peculiar crystals is shown, presenting two hexagonal orientations and obtained on both types of samples, which confirms such a formation mechanism. Moreover, by applying a pretreatment step with different time durations of inductive coupling radiofrequency argon plasma, for which the incident ion energy decreases at 12 eV, uniform coverage of the surface can be achieved with an influence on the density and size of the GHPs.

1 INTRODUCTION–

Since the discovery of fullerenes synthesis[1], sp^2-hybridized carbon nanostructures have been a growing field of interest throughout the scientific community[2]. On this constantly expanding list, one could cite carbon nanotubes[3], graphene[4] but also nanocones[5-6] and polyhedral crystals[7]. However, their synthesis may be a challenge as industrial applications often require defect-free and sizable crystals, two antagonistic parameters[8]. The synthesis of vertically-aligned carbon nanostructures (VACNs) is a good alternative as substrates homogeneously covered with such structures may exhibit interesting properties (*e.g.* light polarization, high thermal and electrical conductivities, high tensile strengths and field

[*]Corresponding author. Tel: +33 (0)3 83 68 47 09. E-mail: ludovic.depoucques@univ-lorraine.fr (Ludovic de Poucques)

emission enhancement[9-10]). VACNs are usually synthesized by plasma treatment, either using a deposition[10-11] or an etching[12-15] process.

Recently, graphite hexagonal pyramids (GHPs, a new type of graphite crystals) have been synthesized on flexible graphite (FG, figure 1(a,b)) and highly-ordered pyrolytic graphite (HOPG) substrates[16]. We suggested a formation mechanism by a plasma etching process. In the present work, new evidences supporting this assumption are shown on both types of samples. Also, by varying the incident argon ion energy, it is possible to affect the surface structuration of HOPG substrates and create arrays of GHPs with a control of their mean density and size. Such results are of great importance as it permits to use surface characterization techniques regardless of their spatial resolution. For example, in a low spatial resolution technique (X-ray diffraction, Raman spectroscopy, field emission measurements), the graphite substrate would drown the signal response of a few randomly scattered GHPs. On the contrary, in a spatially resolved diagnostic with no microscopy feedback (near-edge X-ray absorption fine structure, tip-enhanced Raman spectroscopy), the search for a single nanocrystal would be tremendously time-consuming. A homogenously covered 1x1 cm^2 substrate allows all these techniques to be carried out in order to uncover the physical properties of these new VACNs. Amongst several applications, GHPs could be a good candidate for future field emitters as such geometrical configuration has been proven very efficient in other materials, in particular in micrometric ZnS hexagonal pyramids[17].

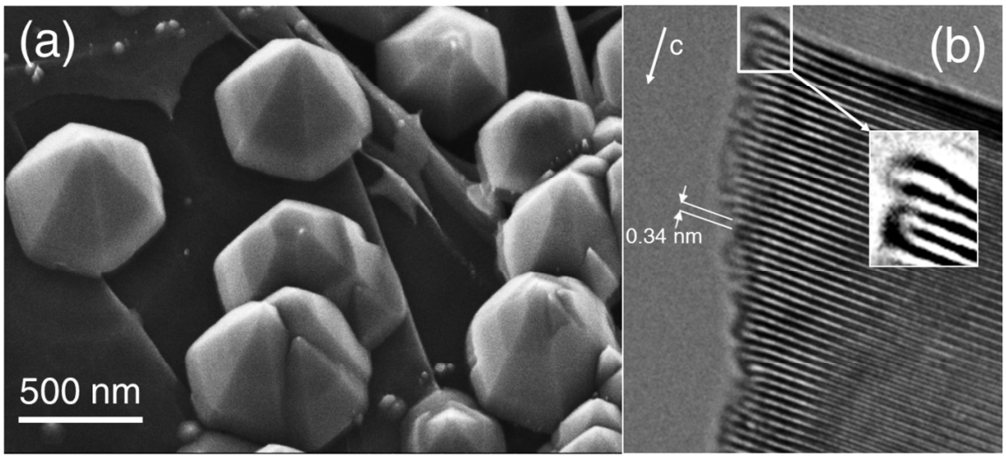

Figure 1. (a) GHPs on a FG substrate[16]. (b) High resolution transmission electron micrograph of the flank of a FG GHP exhibiting loops closing the graphite 002 planes (adapted from Ref. 16). The *c* axis of the graphite lattice is displayed when possible.

2 METHODS–

A– EXPERIMENTAL SET-UP

The experimental set-up is described in details in our previous papers[16,18-20]. To summarize, the GHPs are synthesized from two different graphite substrates: FG and HOPG (table 1). The internal structure of the latter is schematized in figure 2(a). Substrates are treated in a standard helicon reactor with a Boswell-type antenna operating at 13.56 MHz. The plasma is created in a Pyrex chamber and diffuses towards a stainless steel diffusion chamber. Two sets of copper coils permit to apply the static downward magnetic fields, namely B_{diff} (fixed at 10 mT) and B_s (0 or 14 mT depending on the radiofrequency (rf) coupling mode) in the diffusion and source chambers, respectively. The magnetic field lines are parallel to the cylindrical chambers axis. The substrate lies at the center of the diffusion chamber on an electrically insulated substrate-holder. Before treatment, it is heated at 650 °C during two hours at a pressure of 10^{-3} Pa. The heating process is essential to eliminate absorbed water and oxygen that may otherwise desorb during the plasma irradiation and lead to unwanted chemical etching. Then, argon is injected at a rate of 20 standard cubic centimeters per minute to reach 1.3 Pa before turning on the rf discharge with an injected power of 1800 W. The heating goes on during the treatment and the temperature is monitored by a type-K thermocouple whose hot junction is located 10 mm under the substrate-holder surface. After the plasma is turned off, the temperature is slowly decreased below 100°C at residual pressure before extracting the substrate for *ex situ* analysis.

Substrates are carefully weighed before and after the plasma exposure with an OHAUS scale (0.1 mg precision) to assess the mass loss and etching rate. The samples are observed post-treatment using an FEI XL30-SFEG scanning electron microscope (SEM) with an acceleration voltage V_{acc} comprised between 1 and 1.5 kV.

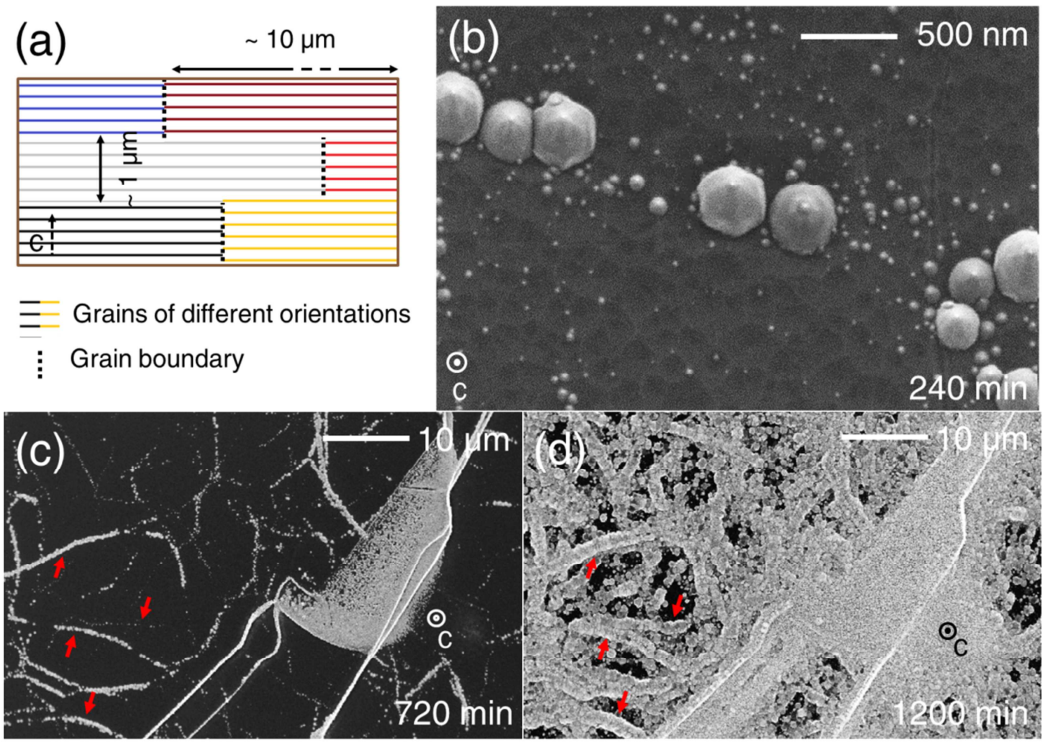

Figure 2. (a) Sketch of the organization of the 002 graphite planes in a typical HOPG substrate. (b,c,d) SEM pictures of GHPs synthesized on HOPG substrates after 4, 12 and 20 hours of plasma treatment, respectively. The red arrows show the alignment of the structures due to their preferential formation on the grain boundaries.

Plasma parameters such as floating (V_f) and plasma (V_p) potentials, electron temperature (T_e) and ion and electron densities ($n_i = n_e$) are estimated by means of a Smartprobe rf compensated Langmuir probe from Scientific Systems Ltd. Measurements were made a few mm above the substrate-holder in the transverse configuration, *i.e.* with the probe length perpendicular to the magnetic field lines, in order to limit the reduction of electronic surface collection due to the charged particles' inclination to follow the magnetic field lines[22]. According to Godyak and Demidov[23], the Druyvesteyn method may still be relevant in our plasma conditions (B_{diff} = 0.01 T, electron temperature $T_{e,min}$ ~ 2 eV) with the chosen probe radius (0.15 mm) and length (1 mm) in the perpendicular orientation. Assessing V_p and V_f permits to determine the argon ions mean energy $E_{ion} = V_p - V_f$ interacting with the graphite substrates at the floating potential (insulated substrate-holder). It has to be noted that the ion energy distribution function is usually not monoenergetic. In fact, in our conditions the ion transit time in the sheath is about a

third of an rf period. In such case, the final ion energy depends on the plasma potential – which oscillates at the rf frequency– during its crossing of the sheath[24]. However, the substrates are located in the diffusion chamber far from the rf power absorption limiting the amplitude of the V_p oscillations. For the sake of simplicity, the latter are neglected and the incident ion energies are approximated to their mean value $E_{ion} = V_p - V_f$.

	Size (mm^3)	Density	Purity	Mosaicity (°)	*ab* domain size	*c* domain size
FG	20×20×0.125	1.2†	99.8‡	3.5±1.5‡	30-40 nm‡	< 2 µm†
HOPG	10×10×2	2.26‡	99.99‡	0.8±0.2‡	<10 µm‡	0.1-1 µm[21]

†Determined experimentally. ‡Manufacturer (Goodfellow SARL) data. [21]See references.

Table 1. Properties of the substrates used for GHP synthesis.

Also, the knowledge of the mass loss (Δm) as well as the ion density and electron temperature allows for the estimation of the etching yield Y according to:

$$Y = \frac{n_C}{n_{Ar^+}} = \frac{\Delta m\, N_A}{M_C} \cdot \frac{1}{S\, t_{pl}\, \phi_i} \quad (1)$$

with N_A the Avogadro number, M_C the carbon molar mass, S the surface exposed to the plasma, t_{pl} the treatment duration, Δm the mass loss and $\phi_i = e^{-0.5} n_e \sqrt{\frac{q\, T_e}{m_i}}$ the ion flux[25] where q is the elementary charge, m_i the argon ion mass and T_e the electron temperature (in eV).

B– RF COUPLING MODES

Plasma treatments are carried out in the so called inductive (IND) or helicon+Trivelpiece-Gould (HEL+TG) rf coupling modes. Such modes are extensively described elsewhere[19,25-26]. Briefly, the rf current flowing through a loop (the Boswell antenna can be seen as a two-loop antenna) induces an oscillating axial magnetic field leading to an azimuthal electric field. This latter may be efficiently absorbed in the presence of a sufficient electron density and drives high inductive currents flowing inside the plasma; this is the inductive mode. Besides, an antenna excited by an rf current is also an electromagnetic field emitter. In IND mode, the dispersion equation of the medium forbids the propagation of these waves in typical conditions[25]. However, by

introducing an external magnetic field (B_s), the dispersion equation changes to allow the propagation of whistler waves, *i.e.* helicon and Trivelpiece-Gould waves, generating the HEL+TG mode in our conditions. This coupling mode is identified in argon gas by a thin blue plasma column impinging on the substrate[16].

3 RESULTS AND DISCUSSIONS–

A– PLASMA CONDITIONS

In order to characterize the formation conditions, Langmuir probe measurements have been carefully performed in the IND and HEL+TG plasma configurations. The results on FG substrates are summarized in table 2. As expected, since substrates are at V_f, the measured E_{ion} show mean values (12 and 25 eV) way below the sputtering threshold. Indeed, for the couple "argon ion/graphite substrate" the sputtering threshold is around 56 eV[27]. The latter is defined as the minimum energy require for one argon ion incoming perpendicularly to the surface so that it has a probability to cause the ejection of a carbon atom from the substrate (with a sputtering yield Y about 10^{-5} atom/ion at $E_{ion} \approx 60$ eV[27]). Sputtering is thus a direct etching process which can be neglected in this study.

	E_{ion} (eV)	$T_{max,C}$ (eV)	ϕ_i (m^{-2} s^{-1})	Etching rate (μm h^{-1})	Etching yield (%)
HEL+TG	25	18	8 10^{20}	0.9	1.9
IND	12	9	13 10^{20}	0.55	0.6

Table 2. Ions, electrons and etching properties of the two rf coupling modes used during the treatments on FG.

The ejected matter is, at E_{ion} = 12 and 25 eV, due to a multi-step process known as ion irradiation induced damage (I3D)[16,28-29] which roughly comes down to a first ion creating damage inside the substrate known as interstitials or adatoms. The former are defined as carbon atoms ejected from the graphite lattice but still contained between 002 planes (also called *ab* planes) whereas the latter relate to carbon atoms lying on the surface of the substrate. Then, another ion can easily desorb these weakly bounded

atoms by knock-on collision. This process is dominating at E_{ion} below the sputtering threshold but high enough to transmit to a carbon atom an energy $T_{max,C}$ greater than the threshold displacement energy of graphite ($T_{d,graph}$ = 15-20 eV[28]). In the case of argon ions impinging on graphite at normal incidence, $T_{max,C} = 0.71 \cdot E_{ion}$[29]. The value of $T_{d,graph}$ explains why, even if the ion flux is 60% greater in IND, the resulting etching yield in HEL+TG at 25 eV ($T_{max,C}$ = 18 eV) is three times higher than the one of IND at 12 eV ($T_{max,C}$ = 9 eV). One may wonder how matter may be etched in the inductive mode if $T_{max,C} < T_{d,graph}$. Two explanations may be suggested. Firstly, measured under electron[28] or ion beam irradiation[29], are reduced under plasma conditions since other energetic species such as metastable states (~ 11.5 eV for Ar^m), electrons and photons interact with the surface[31]. A synergetic effect is often pointed out even if it is not clearly understood. Besides, our results concern plasma treatments on FG substrates whereas $T_{d,graph}$ measurements were obtained on highly ordered graphite crystals[28,30]. On the contrary, FG contains a significant density of etching-enhancing defects (flake edges, steps[16]) where carbon atoms are weakly bound to the graphite lattice, facilitating their desorption. On HOPG, where the density of defects is much lower, the estimated etching rate in the HEL+TG mode is around 0.3 $\mu m \cdot h^{-1}$. In IND mode, the measured Δm after 6 hours of plasma treatment was below the detection limit (precision of the scale) meaning that the etching rate is less than 0.07 $\mu m \cdot h^{-1}$. Both interpretations also explain the high etching yield that is obtained (see table 2), even at E_{ion} way below the sputtering threshold.

B– FORMATION MECHANISM

A formation mechanism of the GHPs at E_{ion} = 25 eV (figure 1(a)) has been proposed and was described in our previous paper[16]. It was assumed to be due to a local etching variation induced by the impurities and topographical defects of the substrates (steps, flake edges in FG and grain boundaries (GBs) in HOPG) leading to the creation of graphite nano-islands and subsequent formation of single loops between the non-terminated graphite planes, as seen in figure 1(b). These loops supposedly resist the I3D better than the graphite ($T_{d,loop} > T_{d,graph}$) and induce the formation of GHPs. This whole formation mechanism of the GHPs has been deduced from the apparent unfeasibility to form highly ordered graphite structures from deposition and/or adatoms arrangement processes at the relatively low surface temperature of 650°C.

The formation of loops is commonly observed in high-temperature treatment of graphite or few-layer-graphene under neutral atmosphere[32]. In these conditions, unterminated adjacent *ab* planes minimize their surface energy by zipping their edges[33]. Such a configuration is metastable –energy has to be brought– but appears to be astonishingly resistant under high temperature treatment which is attributed to the absence of dangling bonds (elimination of free edges). In our conditions, the surface temperature of only 650°C is not sufficient to induce the formation of loops[34]. This means that the latter may not be formed after the plasma treatment but has to be formed during the ion irradiation. Note that the formation of spherical or tubular structures under electron or ion irradiation has been already observed, for example, irradiating a graphene sheet with an electron beam at 80 kV may lead to the formation of C_{60}[35]. One has to note that the loops are at the surface of each pyramids, thus, are directly exposed to the ion irradiation. A formation due to an etching mechanism implies that they are more resistant to the I3D than the surrounding graphite. Although the exact explanation of their resilience is not known at present, some assumptions may be advanced. As already observed[16], a trenching effect increases the local etching in the vicinity of the pyramids, creating free edges sensitive to the ion irradiation. Besides, as in fullerenes[36], the *ab* plane curvature in the loop probably makes it electronegative. Thus, loops would have electron-rich "inside" leading to an electron depletion on the surface and increasing the ion reflection probability. The resilience of the loops may also be greater than the graphite one due to their half-nanotube geometry. Indeed, nanotubes have the ability to reconstruct themselves under ion or electron irradiation[29]. The interstitial created by the I3D process would then be trapped within the loop and recombine with a vacancy in the vicinity. Finally, a vast majority of the loops, observed by HRTEM imaging[16], have diameter below 0.4 nm, which is the smallest value possible for a defect-free nanotube[37,38]. This implies the presence of defects, such as pentagon cycle of sp^3-hybridized carbon atoms that may increase the displacement energy threshold of the loop.

The formation of the GHPs in the HEL+TG mode has been further studied on HOPG. The resulting crystals are presented in figure 2. The hexagonal configuration is slightly misshapen as compared to the pyramids obtained on FG. This could be due to the

roughness brought by the ion irradiation (figure 2(b)) as no roughness was observed before the plasma treatment. Moreover, red arrows in figure 2(c,d) point out different groups of aligned structures. To explain this spatial configuration, one has to recall that the GHPs are coherently oriented with the graphite flake or grain supporting them (crystals and substrate share the same *c* axis[16]). In figure 3(a), the structures show a 10° angle difference in their respective orientation. This proves that they are formed on two different grains with two orientations and that the lines of structures (red arrows in figure 2(c,d) and dotted yellow line in figure 3(a)) reveal the GBs between graphite grains. The preferential formation at GBs is illustrated by the sketch of figure 3(c) which depicts a cross section of the HOPG substrate along the *c* axis, before (t_0) and after ($t = t_1$ or t_2) plasma exposure. At $t = t_1$, argon ions partly eroded the substrate and formed GHPs with a specific orientation on the left side of the GB and GHPs with another orientation on its right. Such a formation would occur either with a deposition or an etching mechanism. However, the occurrence of crystals with two different orientations (2-O) along their *c* axis (rotation of ~30° in figure 3(b)) confirms the previously proposed formation process by means of physical etching with argon ions. Indeed, if a crystal is deposited with a specific orientation, a sudden and complete switch to another orientation is not energetically favorable, excluding a formation by adatoms diffusion and subsequent clustering. Nonetheless, it can be explained by an etching mechanism combined with the intrinsic internal structure of the HOPG. The process is illustrated in figure 3(c), where, at time $t = t_1$, a GHP has been formed on a now eroded grain with a specific orientation (e. g. a blue GHP). This crystal, coherently oriented with the blue grain, resists etching better than the substrate and protects the graphite (gray grain) underneath it. This gray grain has its own orientation which may be different from the blue grain and thus leads to a 2-O GHP: blue orientation on top and gray orientation at the bottom ($t = t_2$). It is the authors' opinion that the occurrence of 2-O crystals is a reliable evidence that they originate from an etching process.

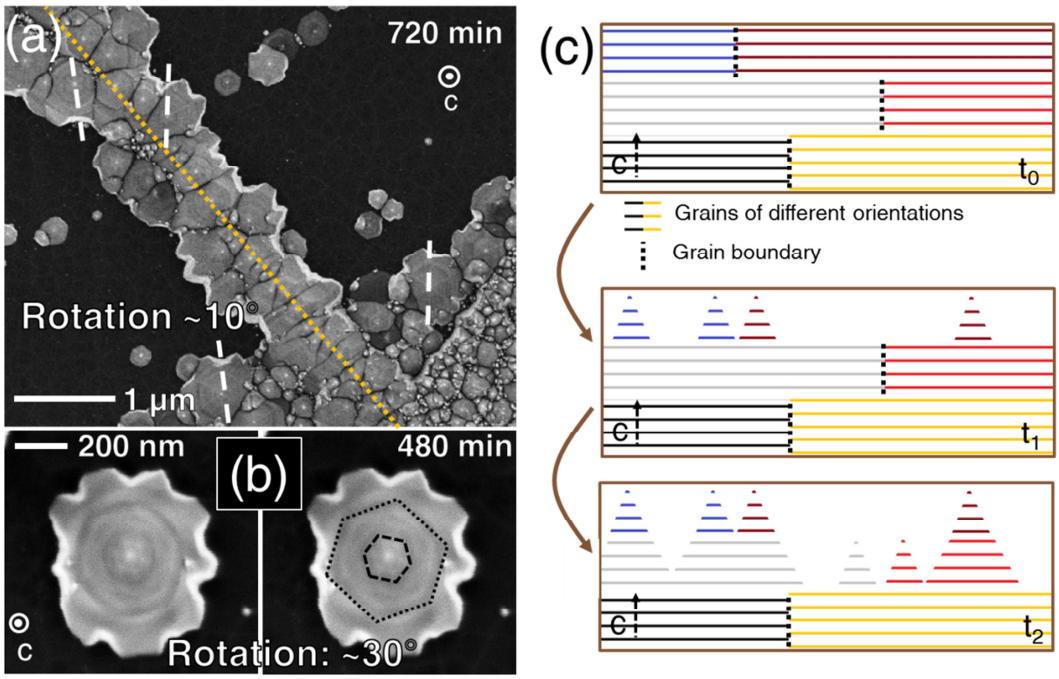

Figure 3 The GHP formation on HOPG. (a) Formation on either side of the GB (dotted yellow line) with a 10° angle between the crystals orientations on the left and on the right of the GB (dashed lines). (b) Isolated crystal with two different orientations (2-O) along its *c* axis, highlighted by the drawn hexagons. (c) Sketch of the temporal evolution of GHP on HOPG via an etching process at 3 different times; t_0 to t_1 explains part (a) and t_1 to t_2 is relevant to part (b).

C– CONTROL OVER CRYSTALS SIZE AND DENSITY

Some treatments were carried out in the IND mode to observe the effects of plasma exposure at an ion energy of only 12 eV ($T_{max,C}$ = 9 eV). Results on FG are presented in figure 4. As recently reported in the HEL+TG mode[16] (E_{ion} = 25 eV), the synthesized VACNs have a size distribution between 50 to 800 nm and the same hexagonal-pyramidal configuration with a relatively constant apex angle –the total angle at the summit of the pyramid– distribution centered around 40° in the IND mode. One would have expected it to change with the ion energy as previously observed in carbon nanostructures synthesis via plasma etching[14]. This means that this angle is associated with the material itself and, at these low values of incident ion energy, not the conditions of irradiation. This goes along with the assumed link between the apex angle and the loops closing the graphite planes on the surface of the GHPs[16]. At E_{ion} = 12 eV, the crystals also appear on large graphite flakes (figure 4(a)). However, contrary to the FG substrates treated in HEL+TG mode, the flake surface is not smooth (figure 1(a)) but entirely covered with nanotips causing a high roughness (figure 4(b,c)). Such a phenomenon has already been observed by Peng *et al.*[39] on diamond-like carbon film ion-irradiated at $T_{max,C} < T_{d,dlc}$. The fact that the nanotips are spread throughout the whole

sample indicates a different formation mechanism, not associated with preexisting surface defects. In the IND mode, the ion density is 3 times higher but the mean energy of the ions E_{ion} is below $T_{d,graph}$, affecting only the extreme surface or weakly-bounded edge atoms. Thus, surface processes, such as adatom diffusion and subsequent clustering are expected to grow more important[39]. This could induce the creation of surface defects (carbon clusters), temporary sustaining the 12-eV I3D, affecting locally the etching and explaining the formation of the nanotips. At E_{ion} = 25 eV, these clusters would be etched away readily leading to a smooth surface. Moreover, as seen on HOPG (figure 3(b)), two orientations are sometimes observed along the *c* axis of some crystals (figure 4(d)), confirming again a formation by an etching mechanism. An additional 40-minute plasma treatment at 25 eV (figure 4(e)) on the same sample shows two interesting results. Firstly, one may notice that the 2-O GHPs are etched by the ion irradiation as the diameter of the top orientation is reduced from 240 to 210 nm (insets of figure 4(d,e)). Considering a 40° apex angle, the resulting etching rate (along c axis) of the GHPs is estimated at 0.06 $\mu m \cdot h^{-1}$. This value is 15 times less than the average rate on the FG samples and 5 times less than the one on the HOPG substrates, thus revealing the strong etching resilience of the GHPs –and thus of the loops– at the relatively low E_{ion} of 25 eV. Secondly, the topography of the analyzed zone has hardly changed after the second plasma treatment. This means that the nanotips (or roughness) formed by the 12-eV ion irradiation are mostly stable under the 25-eV one. One may distinguish a reorganization of the smallest structures (e.g. underlined within the dashed outlines) leading to a slight decrease of their density and increase of their size. As it has been previously suggested, the formation of GHPs can be associated with the number of loops closing the edge graphite planes and resisting the etching[16]. This assumption corroborates these findings as, from all the crystals formed at 12 eV, the bigger ones are more likely to contain numerous loops withstanding the 25-eV ion irradiation.

The link between crystal size and etching resilience is essential in order to influence

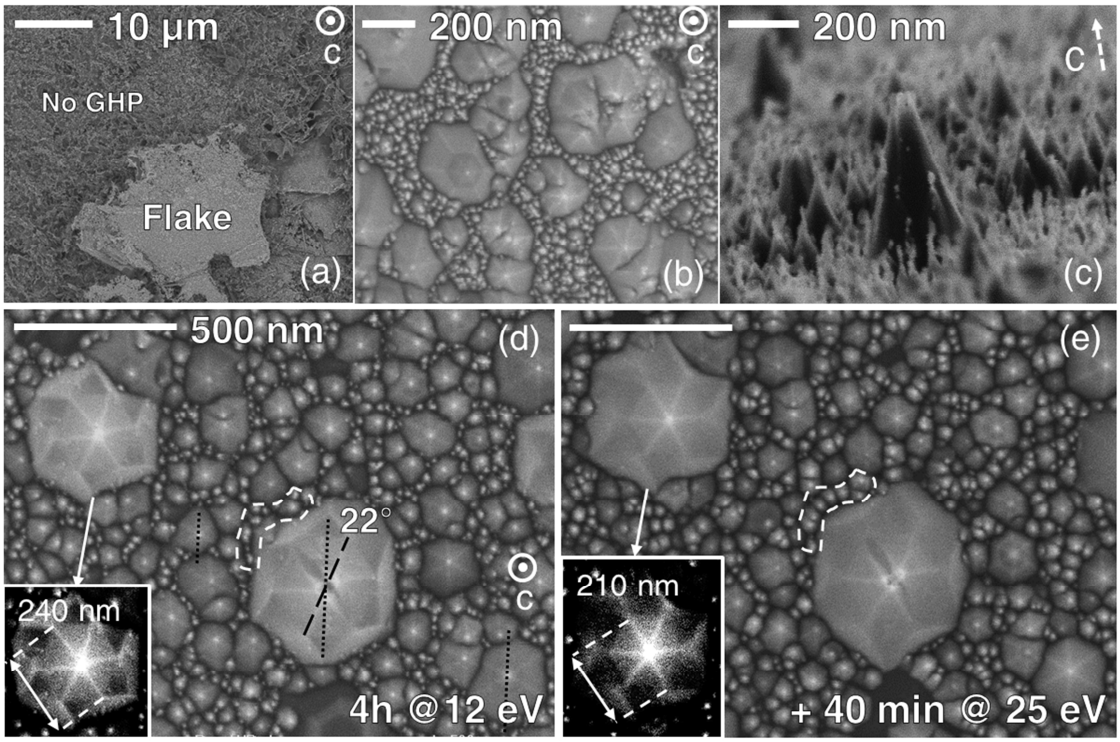

Figure 4 SEM images of FG after a 4-hour plasma treatment in the IND mode (a-d) plus 40 min in the HEL+TG mode (e)**.** (c) permits to observe the relatively constant apex angle distribution (centered around 40°) of the GHPs formed in IND mode. (d) and (e) are taken at the same substrate location. The highly contrasted insets highlight the top orientation of the 2-O crystal.

the mean density of the GHPs. On HOPG, plasma exposure in the IND mode results in a total coverage of the substrate with nanotips (not pictured). The density of which seems independent of the duration of the 12-eV pre-treatment (PT). The latter only influences the size of the tips. With longer PT comes greater –and presumably more resilient to the etching– nanotips. Thus, the idea is to vary the duration of the PT to modify their probability to resist the 25-eV ion irradiation (standard treatment, ST). The results are shown in figure 5. SEM images describe the typical topography of 3 distinctive samples, which were subjected to 3 different PT durations then to a 4-hour ST, as detailed in the figure. Each micrograph is representative of the whole surface, *i.e.* it is entirely covered with the same GHP density. Such results were never obtained before as crystals are preferentially formed on thick and step-rich flakes on FG or at GBs on HOPG. Without this PT, they were previously randomly synthesized throughout the substrate

necessitating the use of SEM imaging to locate the GHPs. A homogenously covered substrate is of great importance because it becomes possible to characterize their physical properties without micrometric resolution. This also permits the use of spatially resolved methods that cannot be coupled with SEM such as field emission techniques, near edge X-ray absorption fine structure spectroscopy or tip-enhanced Raman spectroscopy.

For the sake of assessing the density and size distribution of the structures throughout the substrates, image analysis has been performed using the *Analyze particles* command of the software *ImageJ*[40]. To distinguish each crystal (see red insets in figure 5), a meticulous procedure has been applied following the one described by Papadopulos *et*

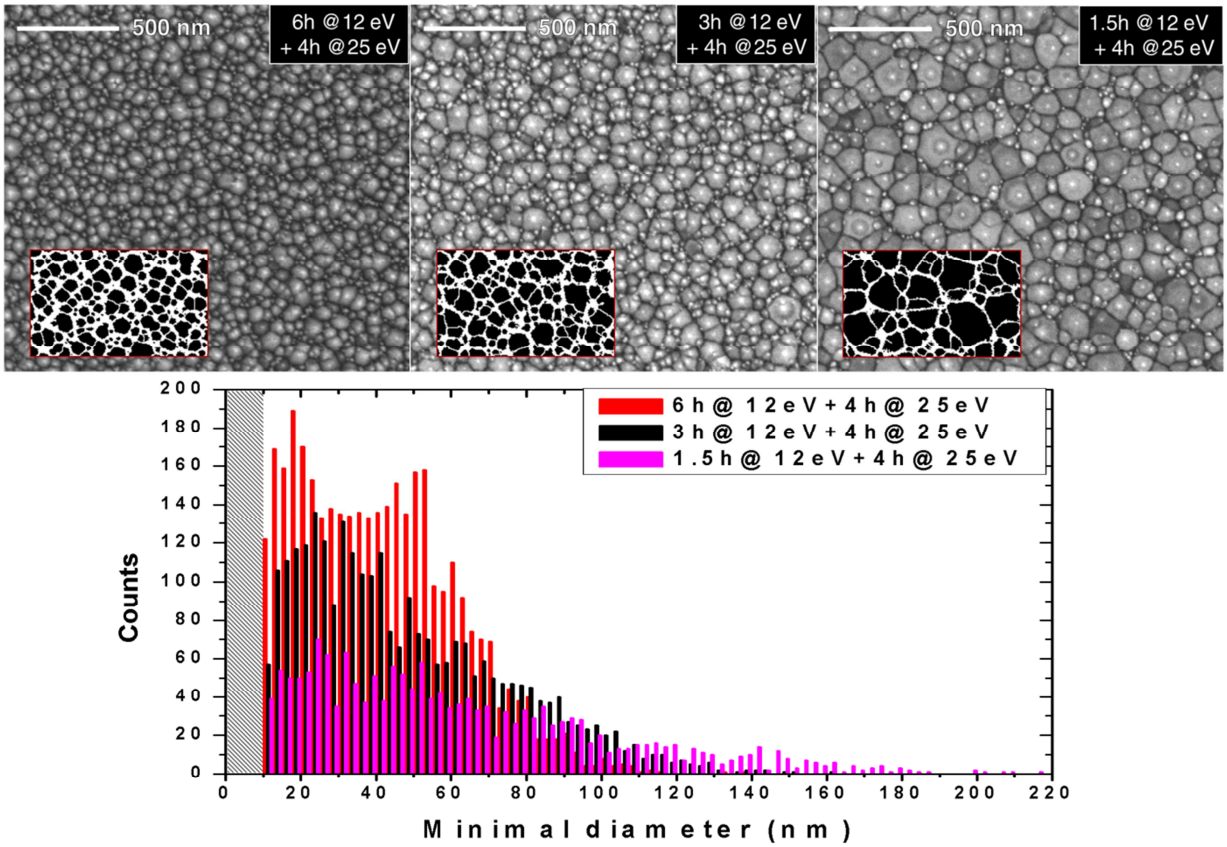

Figure 5 Micrographs of HOPG substrates treated with different plasma conditions and durations. Red insets show respective image segmentation performed with the *Threshold* and *Watershed* commands on ImageJ (GHPs appear in black). The size distribution of the VACNs obtained via the *Analyze particles* command is displayed in the histogram for diameters above 10 nm.

al.[41]. Briefly, the *Threshold* and *Watershed* ImageJ commands are combined to segment the pictures. Then, the *Analyze particles* command provides the number of pyramids and

their area. It should be noted that due to the darker outline of the crystal and because a grey value threshold needs to be set, the resulting area of each particle is slightly minimized. From this measurement, the minimal diameter of each crystal has been estimated assuming a circular geometry. The results, covering 11.6 µm² per sample, are presented in the histogram of figure 5 and summarized in table 3. Diameters below 10 nm are excluded from the data as it would be irrelevant on account of the SEM images resolution (18 nm²/pixel). The X% percentile means that X% of all the GHPs taken into consideration have a diameter below the given value. The image analyses show that, the shorter the PT is, the lesser becomes the density of GHPs after subsequent ST at 25 eV. Also, decreasing the PT duration implies the broadening of the distribution towards greater diameters. This can be explained by the fact that a short PT leads to smaller nanotips (formed under the 12-eV irradiation). Their resilience to the subsequent ST at 25 eV is weak and the resulting density is then reduced during the ST. The remaining GHPs' size increases as their surrounding is etched away. This is coherent with the observations based on figure 4(d,e) where the weakest, *i.e.* smallest, nanotips formed with the PT at 12 eV do not withstand the following 25-eV ion irradiation and are etched away, thus leaving room for the other crystals to expand.

	6h PT + 4h ST	3h PT + 4h ST	1.5h PT + 4h ST
Mean GHP density (μm^{-1})	305	235	145
Minimal diameter range (nm)	10-140	10-160	10-220
- **75% percentile (nm)**	55	65	85
- **90% percentile (nm)**	70	85	115

Table 3. Mean density and size distribution of the GHPs on HOPG substrates regarding different plasma treatments.

4 CONCLUSION–

As previously suggested, new evidences based on the formation of 2-orientations crystals show that graphite hexagonal pyramids are indeed formed by a radiofrequency argon plasma etching process at low pressure, low temperature and low incident ion energy (12 and 25 eV). The main assumption is that surface defects such as steps, flake

edges, impurities and grain boundaries induce during the plasma treatment the creation of carbon loops joining the graphite edge planes which seem to have a higher displacement energy threshold than the rest of the graphite substrate. This results in a local etching rate variation and the formation of vertically aligned nanostructures in localized areas of the sample. Plasma pre-treatments at 12-eV ion irradiation (inductive mode) cause the total and uniform coverage of HOPG substrates with pyramids. Also, varying the pretreatment duration permits to influence the mean density obtained after full treatment and, consequently, the size distribution of the crystals. Therefore, it is now possible to create dense and homogeneous arrays of graphite hexagonal pyramids on large substrates. This marks the first step needed for the characterization, without a visual or imaging feedback, of the physical properties of these new graphite crystals. The new possible surface investigations coupled with a better control of the mean ion energy would shed light on the nature and formation of the loops terminating the graphite edge planes at the surface of the pyramids.

REFERENCES–

1. Kroto H W, Heath J R, O'Brien S C, Curl R F and Smalley R E 1985 *Nature* **318** 162
2. Gogotsi Y and Presser V 2013 *Carbon nanomaterials* (Boca Raton: CRC Press)
3. Iijima S. 1991 *Nature* **354** 56
4. Novoselov K S, Geim A K, Morozov S V, Jiang D, Zhang Y, Dubonos S V, Grigorieva I V and Firsov A A 2004 *Science* **306** 666
5. Lin C-T, Lee C-Y, Chiu H-T and Chin T-S 2007 *Langmuir* **23** 12806
6. Naess S N, Elgsaeter A, Helgesen G and Knudsen K D 2009 *Sci. Technol. Adv. Mater.* **10** 065002
7. Song X, Liu Y and Zhu J. 2007 *Mater. Lett.* **61** 4781
8. Bae S *et al*. 2010 *Nat. Nanotechnol.* **5** 574
9. Jiang K, Wang J, Li Q, Liu L, Liu S and Fan S 2011 *Adv. Mater.* **23** 1154
10. Malesevic A, Kemps R, Vanhulsel A, Chowdhury M P, Volodin A and Van Haesendonck C 2008 *J. Appl. Phys.* **104** 084301
11. Levchenko I, Ostrikov K, Long J D and Xu S 2007 *Appl. Phys. Lett.* **91** 113115
12. Lu X, Huang H, Nemchuk N and Ruoff RS1999 *Appl. Phys. Lett.* **75** 193

13. Choi S, Park H, Lee S and Koh K H 2006 *Thin Solid Films* **513** 31
14. Wang B and Zhang B 2007 *Diam. Relat. Mater.* **16** 1982
15. Muñoz-García J, Vázquez L, Cuerno R, Sánchez-García J A, Castro M and Gago R 2009 *Toward Functional Nanomaterials* ed Z M Wang (New York: Springer) p. 323–98
16. Glad X, de Poucques L, Jaszczak J A, Belmahi M, Ghanbaja J and Bougdira J 2014 *Carbon* **76** 330
17. Chen Z-G *et al.* 2009 *Adv. Funct. Mater.* **19** 484
18. Bieber T, de Poucques L, Vasseur J-L, Hugon R, Belmahi M and Bougdira J *2011Surf. Coat. Technol.* **205** S384
19. Bieber T, Bardin S, Poucques L de, Brochard F, Hugon R, Vasseur J-L and Bougdira J 2011 *Plasma Sources Sci Technol.* **20** 015023
20. Bieber T, Glad X, de Poucques L, Hugon R, Vasseur J-L and Bougdira J 2013 *The Open Plasma Phys. J.* **6** 32
21. Moore A W 1973 *Chem. Phys. Carbon* **11** 69
22. Passoth E, Kudrna P, Csambal C, Behnke J F, Tichý M and Helbig V 1997 *J Phys D: Appl Phys.* **30** 1763
23. Godyak V A and Demidov V I 2011 *J. Phys. D: Appl. Phys.* **44** 233001
24. Barton D, Heason D J, Short R D and Bradley J W 2000 *Meas. Sci. Technol.* **11** 1726
25. Chabert P and Braithwaite N 2011 *Physics of Radio-Frequency Plasmas* (New York: Cambridge University Press)
26. Glad X 2014 *PhD Thesis* Université de Lorraine. Available from : https://hal.archives-ouvertes.fr/tel-01143297 [French]
27. Eckstein W, Stephens J A, Clark R E H, Davis J W, Haasz A A, Vietzke E and Hirooka Y 2001 *Physical sputtering and radiation-enhanced sublimation* ed R E H Clark (Vienna: International Atomic Energy Agency) p. 46
28. Banhart F 1999 *Rep. Prog. Phys.* **62** 1181
29. Krasheninnikov A V and Nordlund K 2010 *J. Appl. Phys.* **107** 071301
30. Marton D, Boyd K J, Lytle T and Rabalais J W. 1993 *Phys. Rev B.* 1993 **48** 6757
31. Rousseau B, Estrade-Szwarckopf H, Thomann A-L and Brault P 2003 *Appl. Phys. A: Mater.* **77** 591
32. Huang J Y, Ding F, Yakobson I, Lu P, Qi L and Li J 2009 *Proc. Nat. Aca. Sci.* **106** 10103
33. Rotkin S and Gogotsi Y 2002 *Mat. Res. Innov.* **5** 191
34. Campos-Delgado J *et al.* 2009 *Chem. Phys. Lett.* **469** 177
35. Chuvilin A, Kaiser U, Bichoutskaia E, Besley N A and Khlobystov A N 2010 *Nature Chem.* **2** 450

36. Haymet A D J 1985 *Chem. Phys. Lett.* **122** 421
37. Qin L C, Zhao X, Hirahara K, Miyamoto Y, Ando Y and Iijima S 2000 *Nature* **408** 50
38. Hayashi T *et al.* 2003 *Nano Lett.* **3** 887
39. Peng X L, Barber Z H and Clyne T W 2001 *Surf. Coat. Technol.* **138** 23
40. http://rsb.info.nih.gov/ij/
41. Papadopulos F, Spinelli M, Valente S, Foroni L, Orrico C, Alviano F and Pasquinelli G 2007 *Ultrastruct. Pathol.* **31** 401